Short communication

Performance and life-time behaviour of NiCu–CGO anodes for the direct electro-oxidation of methane in IT-SOFCs

A. Sin [a], E. Kopnin [a], Y. Dubitsky [a], A. Zaopo [a], A.S. Aricò [b],*,
D. La Rosa [b], L.R. Gullo [b], V. Antonucci [b]

[a] *Pirelli Labs S.p.A., Viale Sarca 222, I-20126 Milan, Italy*
[b] *CNR-ITAE, Via Salita Santa Lucia Sopra Contesse 5, I-98125 Messina, Italy*

Abstract

An anodic cermet of NiCu alloy and gadolinia doped ceria has been investigated for CH_4 electro-oxidation in IT-SOFCs. Polarization curves have been recorded in the temperature range from 650 to 800 °C. A maximum power density of 320 mW cm^{-2} at 800 °C has been obtained in the presence of dry methane in an electrolyte-supported cell. The electrochemical behaviour during 1300 h operation in dry methane and in the presence of redox-cycles has been investigated at 750 °C; variation of the electrochemical properties during these experiments have been interpreted in terms of anode morphology modifications. The methane cracking process at the anode catalyst has been investigated by analysing the oxidative stripping of deposited carbon species.
© 2006 Elsevier B.V. All rights reserved.

1. Introduction

The direct electrochemical oxidation of hydrocarbons in solid oxide fuel cells has recently gained momentum as a promising process for distributed generation of electrical energy. Various anode catalysts have been proposed, including cermets (e.g. Ni alloys or Cu) and, more recently, Mn and Cr-based perovskites [1]. Two main drawbacks have been envisaged, i.e. a lower oxidation rate with respect to hydrogen and the formation of carbon deposits on the anode surface. In this regard, the operating conditions play a fundamental role in determining performance and stability [2,3]. Furthermore, the application of SOFC devices as electrical power systems in the field of distributed generation of energy implies that the anode catalyst should tolerate several redox and thermal cycles [4].

A NiCu alloy/ceria–gadolinia (CGO) composite catalyst offers potential advantages with respect to typical Ni-YSZ (yittria-stabilised zirconia) anode for the direct electrochemical oxidation of hydrocarbons. It has been observed that Cu, as

opposite of Ni, does not catalyse the cracking process; moreover, it is a suitable current collector under anodic conditions [2]. Although a mitigation of the carbon deposition process has been observed in the presence of Ni–Cu alloys [2], it was shown that formation of carbon deposits occurs at 800 °C; yet, as opposite of pure Ni, the formation of carbon fibers on NiCu alloys does not produce an irreversible poisoning of the catalyst and it ameliorates the cell resistance due to an enhanced electronic percolation within the anodic layer [2]. A decrease of operating temperature generally increases the catalyst tolerance towards the cracking process [5]. A reduction of carbon deposits was also observed for unmodified Ni catalysts at low temperatures in the presence of a proper combination of ceria and zirconia electrolytes [5]. This behaviour has been interpreted in terms of enhanced oxygen ion transfer promoted by the doped ceria in combination with the oxygen storage properties of YSZ [5]. Yet, no time-studies have been reported using this approach at intermediate temperatures.

In this work, we have focused our efforts on the investigation of a NiCu alloy–CGO ($Ce_{0.8}Gd_{0.2}O_{1.9}$) catalyst formulation as a suitable combination in terms of catalytic activity and tolerance to carbon deposition. The influence of operating conditions, including temperature, voltage and redox-cycles, on

---

the performance, electrochemical characteristics and prolonged operation behaviour of SOFC devices directly fed with methane has been studied. The carbon deposition under different operating conditions was in situ analysed by monitoring the oxidative stripping of carbon species as CO_2 upon feeding the anode with air.

2. Experimental

The SOFC devices investigated in this study were typical electrolyte-supported button cells of $1 \, cm^2$ active area. They consisted of the following components—anode: Ni–Cu alloy (50 wt.%)/CGO (50 wt.%) cermet (thickness: $15 \, \mu m$); supporting electrolyte membrane: CGO (thickness: $300 \, \mu m$); cathode: $La_{0.6}Sr_{0.4}Fe_{0.8}Co_{0.2}O_{3-\delta}$ (LSFCO, thickness: $15 \, \mu m$).

The synthesis of the CGO powders was carried out by using a co-precipitation method described elsewhere [6,7]. The CGO powder was compacted by uniaxial pressing (300 MPa). The green pellets were treated at $1450 \, ^{\circ}C$ for 3 h in stationary air to obtain a supporting electrolyte membrane ($\rho_{rel} > 95\%$). The LSFCO cathode was deposited by spraying with isopropanol. The deposit was fired at $1100 \, ^{\circ}C$ for 2 h, under stationary air to ensure a good electrode/electrolyte membrane interface. The anode was also deposited by spraying. It consisted of a mixture of CGO and (Ni,Cu)O oxide powders. The NiCuOx powder was synthesized accordingly to the procedure reported in Ref. [8]. The SOFC cells were mounted on alumina tubes, sealed with ceramic adhesive (AREMCO 516) and heated at $700 \, ^{\circ}C$ in air. A gold paste (Hereaus) and gold wires were used to form both anode and cathode current collectors.

The anode was conditioned with helium and H_2; subsequently, it was fed with dry or humidified CH_4 (5% R.H.). The cathode was exposed to stationary air. The electrochemical analysis was performed with a Metrohm Autolab 30 electrochemical apparatus equipped with a FRA and 20 A booster. The exhausting gases from the anode compartment were analysed by a gas chromatograph (Varian, MicroGC). The tolerance to redox-cycles was investigated by switching the anode stream from CH_4 to He and subsequently to air. Afterwards, the cell was directly reconditioned in He and CH_4 without any further use of hydrogen.

Structural and compositional analyses were carried out by XRD (Philips X'pert diffractometer) using a Bragg–Brentano configuration and Cu Kα source. Elemental analysis was carried out by XRF (Explorer, Bruker AXS). Morphology was investigated by SEM (Philips XL30) and TEM (Philips CM12). Surface chemistry was studied by XPS (PHI 5800-01 spectrometer).

3. Results and discussion

3.1. Anode catalyst

XRD and TEM analyses of the NiCuOx catalyst after preparation (Figs. 1 and 2) revealed the presence of a single phase solid solution of NiO and CuO with fcc cubic structure similar to pure NiO (JCPDS 4-835). No evidence of monoclinic CuO (JCPDS 5-661) or amorphous CuOx was detected. As a comparison, the
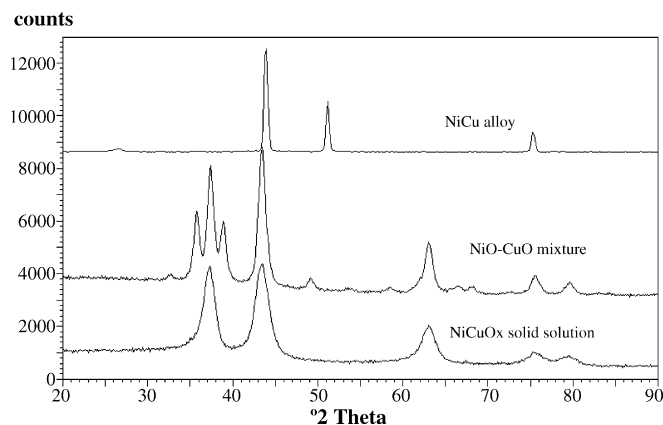

Fig. 1. XRD patterns of a NiCu (60–40 at.%) alloy, NiCuOx solid solution (60 at.% NiO–40 at.% CuO) and NiO–CuO oxide mixture (60 at.% NiO–40 at.% CuO).

catalyst prepared by solid-state reaction of NiO and CuO showed two separate oxide phases (Fig. 1). TEM analysis of the NiCuOx sample showed the presence of nanocrystalline particles of size ranging between 3 and 8 nm (Fig. 2). After reduction at $700 \, ^{\circ}C$ in hydrogen, a NiCu alloy was formed (Fig. 1). XRF analysis of the alloy indicated an atomic bulk composition corresponding to $Ni_{58}Cu_{42}$. The physico-chemical properties of the CGO electrolyte membrane and powders have been reported elsewhere [7].

3.2. Life-time behaviour

In the life-time experiments, the SOFC anode was first conditioned with hydrogen; subsequently, dry methane was fed to the cell. The cell was operated at $750 \, ^{\circ}C$ and at a constant voltage of 0.6 V. After the cell reached steady-state conditions, several polarizations and ac-impedance measurements were carried out in order to investigate the electrochemical properties. The electrochemical behaviour of the cell was found to vary significantly during the first hours of operation. Accordingly, reliable data concerning with the effect of temperature, potential,
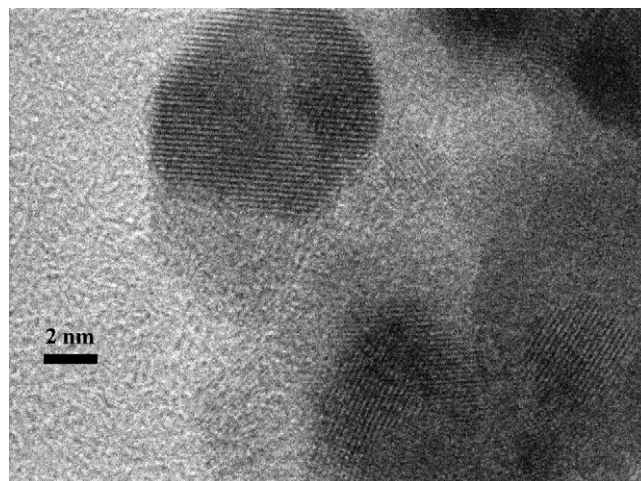

Fig. 2. TEM micrograph with lattice resolution of the 60 at.% NiO–40 at.% CuO nanoparticles.
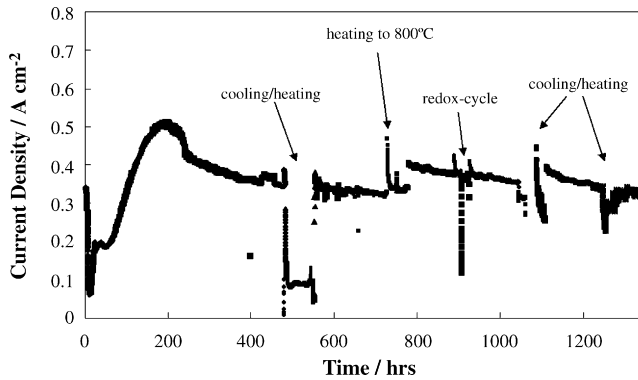
Fig. 3. Chrono-amperometric analysis of the SOFC cell operated at 750 °C, 0.6 V with dry CH_4 fed at the NiCu–CGO anode.
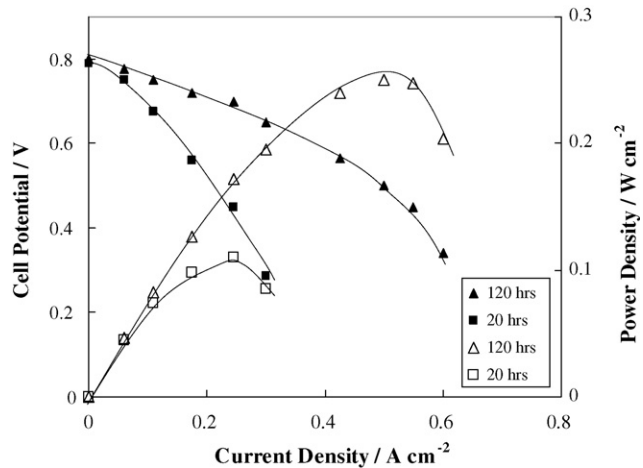
redox-cycles, etc. have been acquired after proper cell conditioning. It was found that after a conditioning period of 300 h, the performance was quite reproducible.

Fig. 3 shows the variation of current density with time (1300 h) at a fixed cell potential (0.6 V). This cell was actually operated for more than 1500 h. For the sake of simplicity, the life-time plot does not include the time elapsed during start-up and shut-down procedures, initial conditioning in hydrogen, experiments made under OCV, polarization and ac-impedance tests at various temperatures. During operation, several specific tests have been carried out, such as thermal and redox-cycles. It was observed that, after switching the anode stream from H_2 to CH_4, the current density initially decreased to 60 mA cm^{-2} and then increased rapidly up to 500 mA cm^{-2}. Subsequently, the current density decreased to 350 mA cm^{-2}, after 350–400 h, and it remained almost constant until the end of the experiment. Although the cell was subjected for short time intervals to thermal/redox-cycles and various electrochemical measurements were carried out, it worked properly during all this period and it was shut-down for analytical purposes only.

In order to monitor morphology changes occurring during operation, several cells were conditioned by using the same procedure reported above; they were shut-down after different periods to be analysed. The performance, obtained after 20 and 120 h of operation, is shown in Fig. 4. A two-fold increase in maximum power density is recorded passing from 20 to 120 h. This evidence was also confirmed by impedance spectroscopy experiments carried out under OCV at three different operating times (Fig. 5). The series (ohmic) resistance (R_s) obtained from the high frequency intercept on the real axis, and the total resistance (R_t) of the cell show a clear improvement with time up to reach steady-state values. R_t is obtained from the low frequency intercept on the real axis and it is attributed to the sum of ohmic and polarization resistances ($R_t = R_s + R_p$) under the present operating conditions.

The polarization resistance (R_p) decreased from about 0.8 to 0.5 Ω cm^2 in the time interval from 20 to 120 h; correspondingly, the ohmic resistance decreased from 1 to about 0.3 Ω cm^2 (Fig. 5). This indicates that both ohmic and polarization resistances decrease with the operation time; but, the reduction of ohmic drop appears more significant.

Fig. 4. Polarization and power density curves after 20 and 120 h operation time at 750 °C with dry CH_4 and stationary air.

SEM analyses have been carried out on the cells shut-down after dry methane operation at different times. Fig. 6 shows the anode layer morphology after 20 and 120 h of operation. It can be clearly observed that the sample shut-down after 20 h is more porous than the sample operated for 120 h (Fig. 6). Therefore, the significant decrease of porosity may have influenced the ohmic properties, as reflected by the decrease of R_s observed by impedance spectroscopy. This might be explained by the increase of the boundary regions between the particles which improves the percolation paths. Since the polarization resistance R_p was also observed to decrease with the operation time (Fig. 5), the loss of porosity did not cause a decrease of the three-phase reaction zone and there was no significant effect on mass transport through the electrode. Thus, it is deduced that the electrocatalytic process improved with time due to an increase of both electronic and ionic percolation paths, as well as, to the increase of the triple-phase boundary region in the presence of a fine porosity. Various attempts have been made in the present investigation to enhance the anode morphology by increasing the firing temperature. Yet, this resulted in a loss of CuO phase by evaporation or in a preferential segregation of Cu on the surface. Such drawbacks have made quite difficult to control the bulk and surface composition in the catalyst layers fired at high temperature (e.g. 1300 °C). From our evidence, a suitable atomic mixing
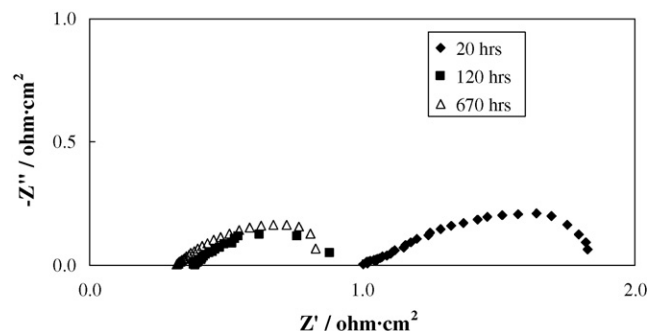

Fig. 5. ac-Impedance spectra at OCV at various operation times at 750 °C with dry CH_4 and stationary air.
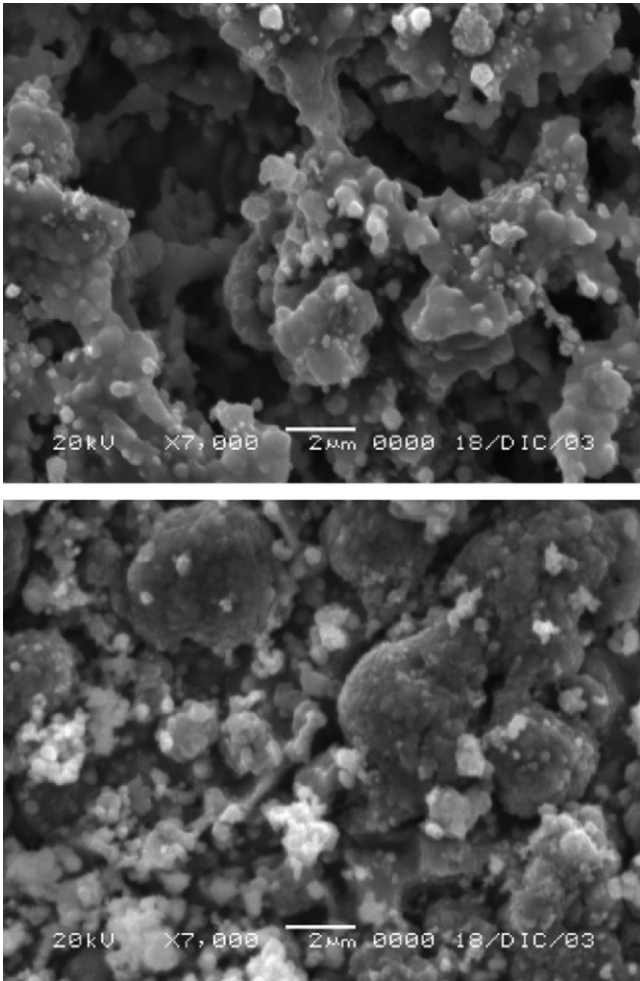
Fig. 6. SEM micrographs of the anode layer after 20 h (top) and 120 h (bottom) operation.

Fig. 7. XPS analyses of the anode layer after 670 h operation before (top) and after (bottom) argon ions sputtering.

3.3. Performance behaviour

A comparison of polarization and power density curves at different temperatures (650–800 °C) after about 500 h of operation (almost steady-state condition) is shown in Fig. 8. The polarization curves show a low open circuit potential but moderate potential losses as a function of the current density at high temperature. This behaviour is suitable for high power regimes. It is also possible to observe that the cell performance increases

between Ni and Cu is a key aspect to achieve a good compromise between proper catalytic activity and mitigation of the carbon deposition process.

The variation of the alloy composition with operation time was investigated by XPS (Fig. 7). The initial surface composition of the alloy revealed a Ni:Cu atomic ratio equal to 1.4 (not shown). After 670 h of operation, an atomic concentration ratio of 21.2 (Ni at.%)/18.7 (Cu at.%) = 1.13 was measured. This indicates the occurrence of a slight surface enrichment of Cu. A further analysis was carried out after sputtering the sample surface with Argon ions (Ar$^+$, 5 kV, 30 mPa extractor pressure) to analyse the composition of the inner layers (Fig. 7b). From this analysis, an atomic ratio of 20.3 (Ni at.%)/14.7 (Cu at.%) = 1.38 was obtained, corresponding to the nominal bulk alloy composition. It is derived that that the Ni–Cu alloy shows a suitable chemical stability under cell operation conditions with a slight Cu surface enrichment after prolonged operation. This may explain the slight decrease of performance passing from 200 to 670 h since it is well known that Ni is catalytically more active than Cu [2,9]. However, copper is necessary to mitigate the carbon deposition on the catalyst surface [2].
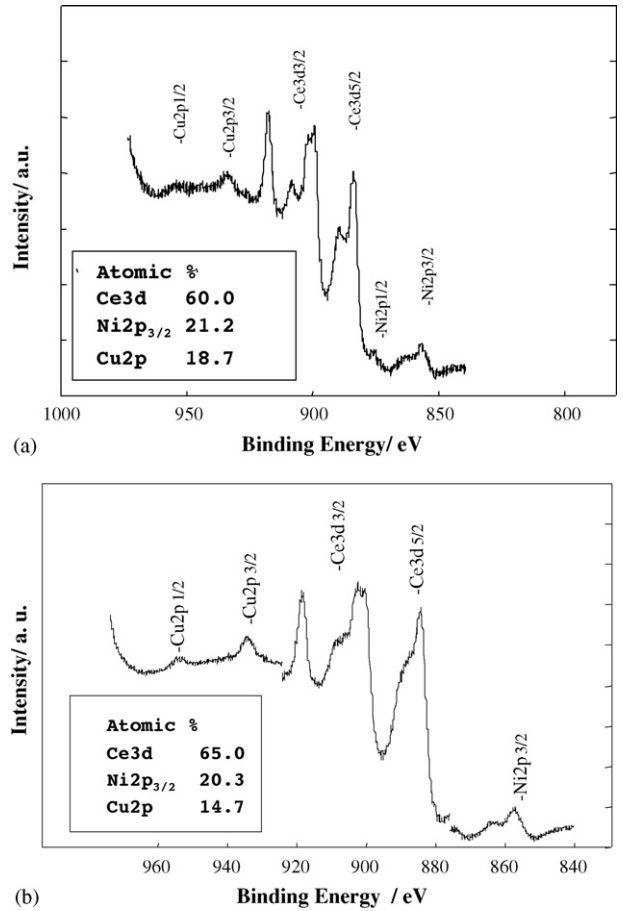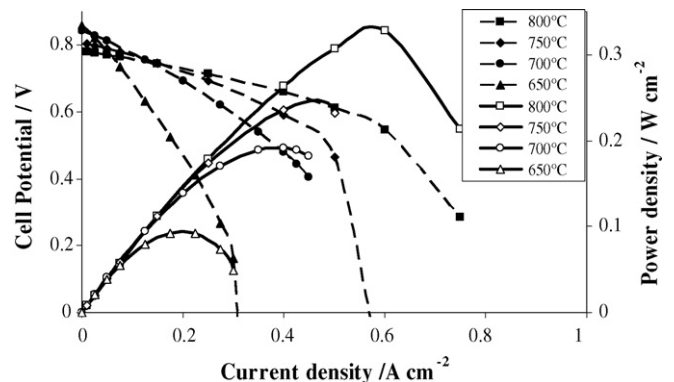

Fig. 8. Polarizations and maximum power densities curves at different temperatures after 500 h operation with dry CH_4 and stationary air.

with temperature, reaching the maximum power density value of $0.320 \, W \, cm^{-2}$ ($0.6 \, A \, cm^{-2}$, $0.54 \, V$) at $800 \, °C$ in the presence of dry methane. The increase of temperature, however, causes a decrease of OCV; this is quite lower than the thermodynamic value. This effect is generally attributed to increase in electronic conductivity in the ceria-based electrolyte due to the $Ce^{4+} \rightarrow Ce^{3+}$ reduction that occurs at high temperatures [10] producing a parasitic drag of electrons through the electrolyte at the open circuit potential [11]. A change in slope of the polarization curves was particularly observed at high temperatures ($750–800 \, °C$) below $0.6 \, V$ (see Figs. 4 and 8). Such a behaviour was not significantly affected by a variation of flow rate at the anode compartment or by air feeding at the cathode instead of stationary air (not shown). It was previously shown that the half-cell characteristic of Ni/SDC anodes for the direct methane oxidation at intermediate temperatures was affected by a concentration polarization resulting from an oxidation rate at the catalyst surface higher than the rate of O^{2-} supply at the triple-phase boundary [9]. A similar situation may occur in the present case since the rate-determining step appears to be related to the anodic process. In fact, small overpotentials ($\sim 0.1 \, V$) were recorded at high currents ($1 \, A \, cm^{-2}$) for the polarization of LSFCO/CGO half-cells with same composition and microstructure [12]. This evidence indicates that further optimization of the anode microstructure is required.

3.4. Investigation of carbon deposits and redox-cycles operation

The carbon deposition during prolonged operation in CH_4 was investigated by carrying out proper redox experiments. The procedure consisted in switching the CH_4 stream to pure He flow for a time sufficient to remove methane from the anode compartment; afterwards, a flux of air ($20 \, cm^3 \, min^{-1}$) was fed to the anode chamber; the exhausting gases were analysed by gas chromatography. The duration of each chromatographic analysis was 3 min. The complete disappearance of the CH_4 signal in the anode outlet after the initial gas switch to He was assumed as an evidence of the complete methane removal. After monitoring the stripping profile of deposited carbon species, as CO_2, He and subsequently CH_4, were fed to the anode to complete the redox-cycle. The analytical procedure here adopted is essentially similar to the oxygen pulses technique generally used in catalytic experiments to investigate the deposition of carbon species on the catalyst surface [13].

The detection of CO_2 at the outlet of the anode compartment for the cell previously operated with dry methane reveals a slight presence of carbon deposits that in contact with O_2 molecules, are combusted at $750 \, °C$ (Fig. 9); however, these species were not found to degrade the cell performance during about $1300 \, h$ operation. Instead, the cell operated with humidified CH_4 ($5\% \, H_2O$) showed a significantly lower amount of carbon deposits (Fig. 9). Yet, superior performances were observed for dry methane operation (about 20% higher power density than in the presence of humidified CH_4, not shown).

Since a pre-requisite of SOFCs for distributed generation of electrical energy is the anode tolerance to redox-cycles, specific
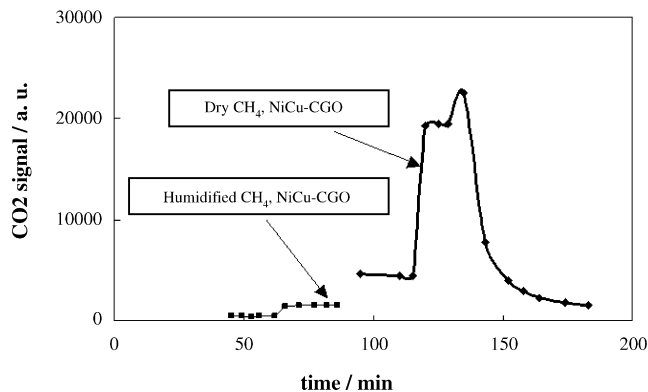

Fig. 9. MicroGC analysis of CO_2 formation due to the oxidative stripping of deposited carbon species for SOFC anodes after operation for about $500–600 \, h$ with dry and humidified methane at $750 \, °C$ and $0.6 \, V$.

experiments were carried out to investigate this effect. In these experiments, the oxidation process was accelerated by flushing the anode with air at $100 \, ml \, min^{-1}$ for about $4–6 \, h$ before purging the anodic compartment with He; subsequently the cell was again fed with dry methane. No hydrogen conditioning was used during these redox-cycles. Fig. 10 shows a chrono-amperometric measurement carried out during several redox-cycles at $0.6 \, V$ and $750 \, °C$. During this experiment, the operating voltage was automatically deselected when an inverted current was passing through the circuit.

It can be observed that the anode was temporarily deactivated when the air flow was fed to the anode compartment during the redox-cycles. However, the system operated quite reversibly, regaining performance after successive exposure to methane. It is important to note that the anode was able to tolerate several cycles in which only CH_4 has been used to reactivate the electrode. Yet, a slight decrease in performance was observed with time (Fig. 10). At present, we cannot quantify how much is the loss of performance due to anode catalyst degradation or to the partial decrease of adhesion between the anode and the gold current collectors (a slight evidence of this latter phenomenon was observed after the cell was shut-down). Further work is being addressed to improve the morphological properties of the anode and to individuate the most proper current collector to enhance the tolerance to redox-cycles.
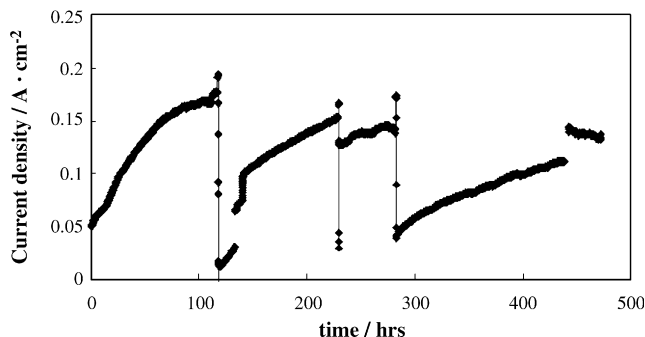

Fig. 10. Chrono-amperometric analysis of the SOFC cell operated at $750 \, °C$, $0.6 \, V$ subjected to various redox-cycles (dry CH_4–He–air–He–dry methane).

4. Conclusions

A NiCu/CGO anode was investigated for the electro-oxidation of dry CH_4. Suitable performance was obtained during about 1300 h operation with an electrolyte-supported cell. It has been observed that a modification of the anode porosity occurring during prolonged operation significantly influences the cell performance. The NiCu alloy composition was not observed to change substantially during the life-time test. An atomic mixing between Ni and Cu appears to be a suitable approach to achieve a good compromise between proper catalytic activity and mitigation of the carbon deposition process. Although the SOFC was sporadically subjected for short time intervals during the life-time test to thermal/redox-cycles, it worked properly. Yet, a decay in performance was observed when redox-cycles of several hours were in sequence applied to the cell. A maximum power density of $0.32\,W\,cm^{-2}$ was recorded at $800\,°C$ with dry methane. The formation of small carbon deposits after prolonged operation did not affect substantially the performance. However, carbon deposition can be minimized by humidifying the anode stream. Further studies are necessary to improve the anode tolerance to redox-cycles and, more generally, to optimize the anode morphology.

References

[1] S. Tao, J.T.S. Irvine, Nat. Mater. 2 (2003) 320.
[2] H. Kim, C. Lu, W.L. Worrell, J.M. Vohs, R.J. Gorte, J. Electrochem. Soc. 149 (2002) A247.
[3] M. Mogensen, K. Kammer, Annu. Rev. Mater. Res. 33 (2003) 321.
[4] J.T.S. Irvine, A. Sauvet, Fuel Cells 1 (2001) 205.
[5] E. Perry Murray, T. Tsai, S.A. Barnett, Nature 400 (1999) 649.
[6] J.V. Herle, T. Horita, T. Kawada, N. Sakai, H. Yokokawa, M. Dokiya, Ceram. Int. 24 (1998) 229.
[7] A. Sin, Y. Dubitsky, A. Zaopo, A.S. Aricò, L.R. Gullo, D. La Rosa, S. Siracusano, V. Antonucci, C. Oliva, O. Ballabio, Solid State Ionics 175 (2004) 361.
[8] A.S. Aricò, L.R. Gullo, D. La Rosa, S. Siracusano, A.B. Lopes Corriera Tavares, A. Sin Xicola, Solid oxide fuel cell, International Patent PCT/EP02/11963.
[9] J.B. Wang, J.C. Jang, T.J. Huang, J. Power Sources 122 (2003) 122.
[10] H.C. Yao, Y.F.Y. Yao, J. Catal. 86 (1984) 254.
[11] B.C.H. Steele, Eur. Fuel Cell News 7 (2000) 16.
[12] A. Sin, A.S. Aricò, L.R. Gullo, D. La Rosa, E. Kopnin, Y. Dubitsky, A. Zaopo, V. Antonucci, in: S.C. Singhal, J. Mizusaki (Eds.), Solid Oxide Fuel Cells IX, vol. 2, Materials, ECS Proceedings 2005–07, 2005, pp. 1658–1666.
[13] J.R. Rostrup-Nielsen, Steam Reforming Catalysts, Danish Technical Press, Copenhagen, 1975.